

Multistage Deep-Drawing with Alternating Blank Draw-In for Springback Reduction in Transfer and Progressive Dies

David Briesenick^{1,a*} and Mathias Liewald^{1,b}

¹Institute for Metal Forming Technology, University of Stuttgart, Germany

^adavid.briesenick@ifu.uni-stuttgart.de, ^bmathias.liewald@ifu.uni-stuttgart.de

*corresponding author

Keywords: High-Strength Steel, Multistage Metal Forming, Springback Compensation.

Abstract. Cold formed sheet metal parts made of advanced high-strength steels (AHSS) offer a high potential for a lightweight, durable and economic design. However, manufacturing dedicated, high-strength parts with cold forming technologies such as conventional deep-drawing often results in unacceptable shape deviations due to elastic springback after unloading the part from the forming tools. Therefore, various springback compensation methods have been established to ensure dimensional quality of such sheet metal parts. At the Institute for Metal Forming Technology (IFU Stuttgart), deep-drawing with alternating blank draw-in was developed in this context as a new approach to reduce springback and enhance cold forming of AHSS sheet metal parts. Presented work provides numerical sensitivity analysis as well as experimental studies about this new forming method. The asymmetric and alternating blank draw-in, which is changed within a multistage forming process sequence, results in an alternated bending over tool radii and leads to a beneficial stress superposition in the part wall area with reduced springback phenomena. Compared to conventional deep-drawn sheet metal components, springback of a benchmark part geometry could thus be reduced over 75 % by a three-stage forming process with an optimized blank draw-in kinematic.

Introduction

The automotive industry today faces increased demands in lightweight design because of new electric driving technologies and emission restrictions. As a result, advanced high-strength-steels (AHSS) are increasingly being used for structural car body parts in order to compensate for additional equipment weight while simultaneously maintaining crashworthiness. However, conventional manufacturing technologies for producing such high-strength parts like sheet metal forming are limited due to the high material strength, which is often accompanied by low formability and a distinct springback behavior [1]. Furthermore, these advanced material properties lead to relatively high process loads for the presses and tools during forming and shear cutting operations, accelerating their wear [2].

Springback phenomena in sheet metal forming applications occur after forming processes when releasing the part from the tool. It is mainly caused by an elastic strain recovery of material after unloading and can significantly affect the dimensional quality of the formed part. Thereby, shape deviations between designed and formed part geometry may vary locally and depend on part geometry, material and forming process [3]. Whereas part geometry and material is specified by the desired shape and part functionality, springback related shape deviations also result from remaining elastic stress fractions and their inhomogeneous distribution, which depend on the yield behavior and material flow during forming process [4]. Research work by ul Hassan et al. [5] identified the strain dependency of Young's modulus and strain hardening as two important and sensitive factors on springback. For these reasons, sophisticated process planning of forming tools and processes require an accurate springback prediction based on proper descriptions of elastic and plastic material properties. Here, the proposed two surface plasticity model by Yoshida et al. [6] combines the strain dependent change of Young's modulus, the kinematic hardening, transient softening and the Bauschinger effect. This model improves accuracy of springback prediction, but the parameter identification requires an increased testing and determining effort [7].

In order to extend the limits of AHSS part production, various methods have recently been developed to overcome the manufacturing-related drawbacks. Here, the direct press hardening of manganese-boron steels belongs to commonly used manufacturing technologies, with forming and hardening being performed in a single operation [8]. However, the press hardening technology reveals considerable deficits compared to cold forming techniques in terms of cycle time and piece cost. For this reason, new approaches for the cold forming of AHSS have been developed. The trim-free sizing deep drawing (smartform) presented by Kibben et al. [9], for example, enable cold forming of U-shaped profiles with a high dimensional accuracy. Furthermore, Radonjic et al. [10] showed a decreasing springback by the modification of a conventional draw bending process of a hat-shaped channel made of DP 980. Here, the material bends back and forth over the tool radii by alternating the draw-in of the two flange sides during the forming stroke. This reduces the high stress difference between the outer and inner fiber of the part, originating from conventional draw bending procedures due to superimposed tension and bending stresses. Besides an implementation in a single tool operation which requires sophisticated hydraulic actuators, multistage deep-drawing with alternating blank draw-in in transfer and progressive dies may offer further potentials in terms of variable tool radii design. In order to benefit from the observed effects for springback compensation in serial production, research investigations about tool and process parameter sensitivities are necessary for an improved process application.

Numerical Tool and Process Parameter Study of Multistage Deep-Drawing

Supported by a numerical parameter study, dominating influences of the multistage deep-drawing with alternated blank draw-in are revealed. The numerical and experimental investigations described in the following were carried out with the dual-phase steel DP980 and a blank thickness t of 0.97 mm. First, a conventional determination of elastic-plastic material properties was done by standardized uniaxial tensile tests [11]. In addition, cyclic tensile and shear tests were performed to determine model parameters of the Yoshida-Uemori kinematic hardening model subsequently. A detailed description of the carried out characterization procedure and further details of yield behavior of investigated DP980 steel can be found in a previous work of the authors [12]. Derived parameters, which are shown in Table 1, were implemented in the LS-DYNA kinematic hardening and transversely anisotropic material model (*MAT_125).

Table 1. Material model parameter of DP980 (sheet metal thickness $t = 0.97$ mm) [12].

Material Properties									
Material	t [mm]	E [GPa]	YS [MPa]	UTS [MPa]	UE	n	R_0	R_{45}	R_{90}
DP980	0.97	205	718.3	1015.7	8.09	0.108	0.84	1.05	0.87
Y-U Model Parameter									
m	RSat	b	B	C	Y	h	$E0$	Ea	ξ
3.3	474.6	629.3	891.4	400	718	0.8	205	159	62.2

Using this material model, a numerical study was carried out to identify dominant sensitivities of tool and process parameters for the multistage deep-drawing with alternating blank draw-in of a simplified hat-shaped part. The rectangular blank to be formed (160 mm x 100 mm x 0.97 mm) was discretized by shell elements with an edge length of 1 mm and seven integration points over blank thickness. The numerical simulation model was set up for LS-DYNA Solver R9.3 with parameterized keyword files. Subsequently, multistage forming simulations were performed, which included the first two operations of deep-drawing with alternating blank draw-in and the springback in-between, as well as the closing shape-set operation and unloading of the final part geometry (see Fig. 1). In the simulation study, tool and process parameters were varied for the two stages of deep-drawing with alternating blank draw-in within a drawing depth (DD) of 35 mm. More specifically, the radii of die and punch in operation 10 and 20 was independently changed in a range between 3 mm and 10 mm by a FE-mesh morphing subroutine implemented in Altair Hypermesh 14.0. Furthermore, the

respective drawing depths of the two deep-drawing operations were varied between 5 mm and 30 mm by defining a drawing depth ratio i_{12} (1) between them.

$$i_{12} = \frac{DD\ I}{DD\ II} = \frac{DD\ I}{35\ \text{mm} - DD\ I} \quad (1)$$

The alternating blank draw-in was achieved by asymmetric blankholder forces, which were applied inversely in each of the first two forming operations. In this respect, a numerical pre-study revealed that a minimum blankholder force per part of 260 kN (≈ 60 MPa initial blankholder pressure) must be applied on the one blankholder side to suppress the draw-in. At the same time, the restraining force on the opposite blankholder side has to be set at 100 kN to ensure sufficient plastification of the sheet metal part and proper contact between blank and tools. The closing shape-set operation, in which the final part geometry is formed, was calculated in all simulations performed with constant punch radii of 5.8 mm and die radii of 6 mm. Furthermore, a symmetric blankholder force of total 800 kN was consistently selected for this final operation, as in this process step the material is stretched and thus the sidewall curls are reduced.

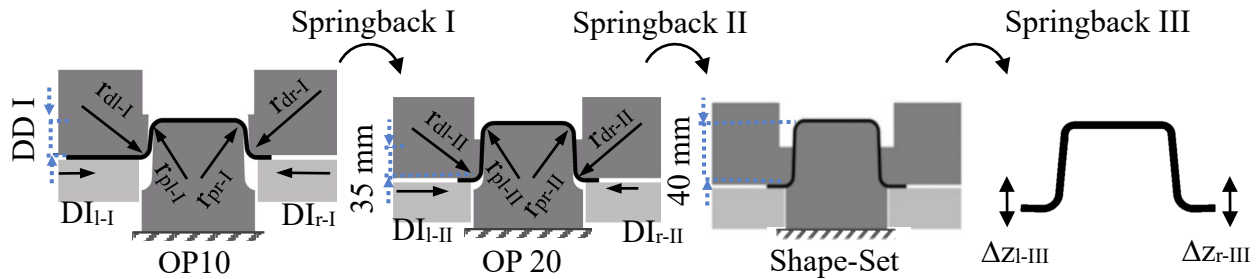


Fig. 1: Multistage forming and springback simulation of deep-drawing with alternating draw-in.

To elaborate sensitivity of investigated process and tool parameters, randomized parameter samplings were selected using the Monte-Carlo method [13], resulting in over 400 simulation runs. Besides the variation of input parameters such as tool radii and drawing depth, flange displacement at the very end of the process (ΔZ_{III}) and the amount of alternating draw-ins ($DI_{I/II}$) was automatically changed for each run and each part side. Complete simulation procedure was implemented and controlled via mathematical optimization tool LS-OPT 6.0 and allowed a determination of percentage influences and correlations. Here, the drawing depth ratio i_{12} showed a dominant impact of 47 % on the alternating draw-in kinematic. On contrary, tool radii of operation 10 and 20 affected the draw-in on the right flange in OP10 (DI_{r-I}) and on the left flange in OP20 (DI_{l-II}) only to a minor extent between 4 % and 12 %. Looking at the resulting shape deviations after springback, represented by the flange displacements ΔZ_{I-III} and ΔZ_{r-III} , the drawing depth ratio i_{12} also revealed as a dominant process parameter. Indicated by a total influence of 36 % on flange displacement, the drawing depth ratio between operation 10 and 20 (i_{12}) impacts the springback compensation effect significantly. Variable designed tool radii showed less effect within the two deep-drawing stages with alternating draw-in by an average influence of 7.5 %. Thus, a neglectable impact of tool radii on forming and springback result can be stated, which allows the use of constant radii and therefore a simplification of the tool and process design.

For the identification of a beneficial process setting within the investigated parameter space, a visualization of the output parameter illustrates a dominant linear correlation between drawing depth ratio i_{12} and the alternating draw-in of deep-drawing operations 10 and 20 (see Fig. 2). Here, the draw-in of OP10 on the right flange side (OP10 DI_{r-I}) and the draw-in of OP20 on the left flange side (OP20 DI_{l-II}) are equal at a drawing depth ratio $i_{12} = 1.6$. This results in a symmetric flange length after forming operation 20 and enables a proper shape-set stage in the final forming operation. Respectively, numerical results propagate neglectable draw-in (< 3 mm) on the opposite clamped flange sides and enables a proper alternating draw-in kinematic of the blank.

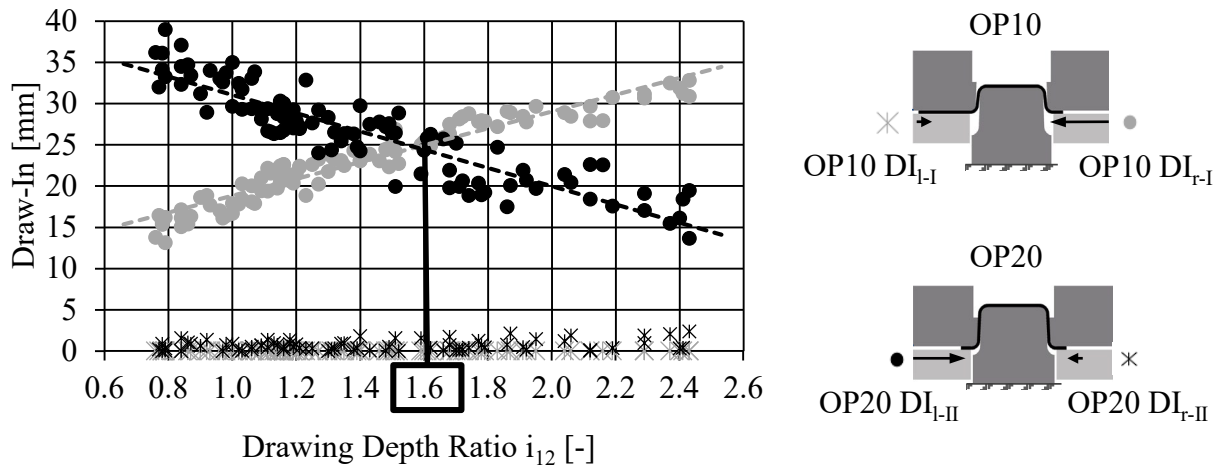


Fig. 2: Numerical results of draw-in for a variable drawing depth ratio within deep-drawing operation 10 and 20 with alternating blank draw-in.

In addition, the springback at the very end of the simulated forming sequence was tracked by the flange displacement on the left (ΔZ_{l-III}) and on the right part side (ΔZ_{r-III}). The results for a variation of tool radii and drawing depth ratio were plotted over the dominant parameter i_{12} (see Fig. 3). It is noticeable that a symmetrical flange length after the first two deep-drawing operations with alternating draw-in is accompanied by a robust springback compensation of the final part geometry. Therefore, a symmetrical and alternating draw-in of the blank within two forming operations overcompensates the scattering of springback due to variable tool radii. Also, it can be observed that the flange displacement ΔZ_{III} generally changes from negative to positive values by an increase of the drawing depth of OP10 (DD I). Due to the superposition of high tensile stresses on the inner part fiber for high drawing depths in OP 20 (DD II), negative sidewall curls occurred and lead to negative flange displacements. In contrast, if the proportion of the drawing depth in the first deep-drawing operation with alternating draw-in (DD I) increases, the tensile stress superposition shifts to the outer part wall fiber and leads to a positive sidewall curl, resulting in positive flange displacements.

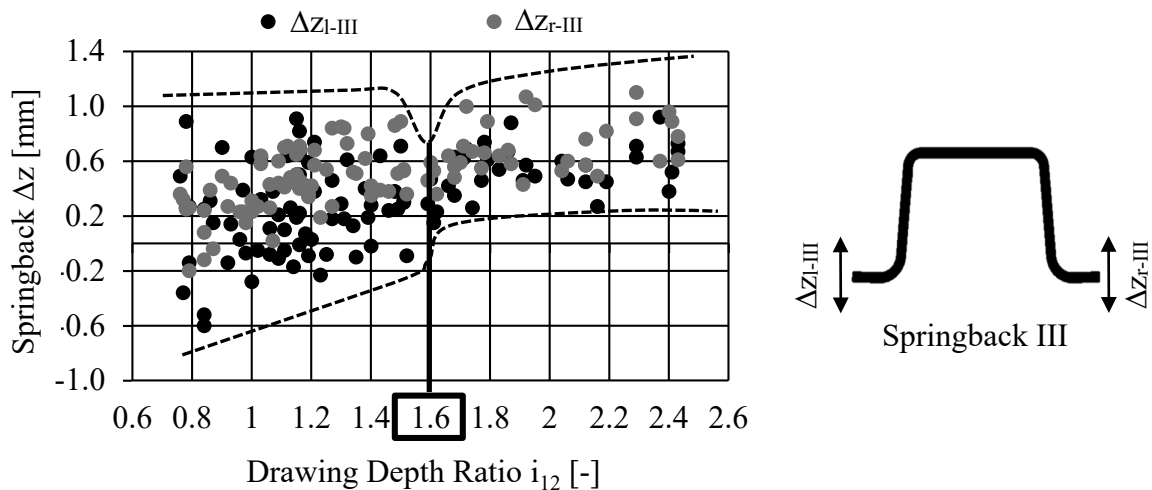


Fig. 3: Numerical springback results of flange displacements after shape-set for a variable drawing depth ratio within deep-drawing operation 10 and 20 with alternating blank draw-in.

Multistage Tool Concept and Experimental Setup

Based on the findings of the aforementioned numerical study on process and tool parameter sensitivity, a multistage tool concept was developed and transferred to an existing prototype tool at the Institute for Metal Forming Technology in Stuttgart. Thus, by a relatively simple modification of the blankholder between each forming operation, multistage deep-drawing with alternating blank

draw-in could be demonstrated on laboratory scale using one single tool. Fig. 4 a) illustrates the lower part of this tool featuring a S-curved punch, a base plate with four pillar guides and a divided blankholder plate with six cushion pins as a support of the two blankholder halves. On both sides, the blank draw-in can be measured by four displacement measurement sensors (SICK OD Mini) using laser triangulation. Additionally, to ensure a reproducible optical measurement by means of part digitization (GOM ATOS 5M) on a clamping device (see Fig. 4 c), two reference holes can be pierced at the end of each formed part by a piercing unit integrated between punch and die (see Fig. 4 b). Using different blank shapes, the tool design allows the forming either of small hat-shaped parts at the straight geometry sections or of the complete S-Rail part geometry.

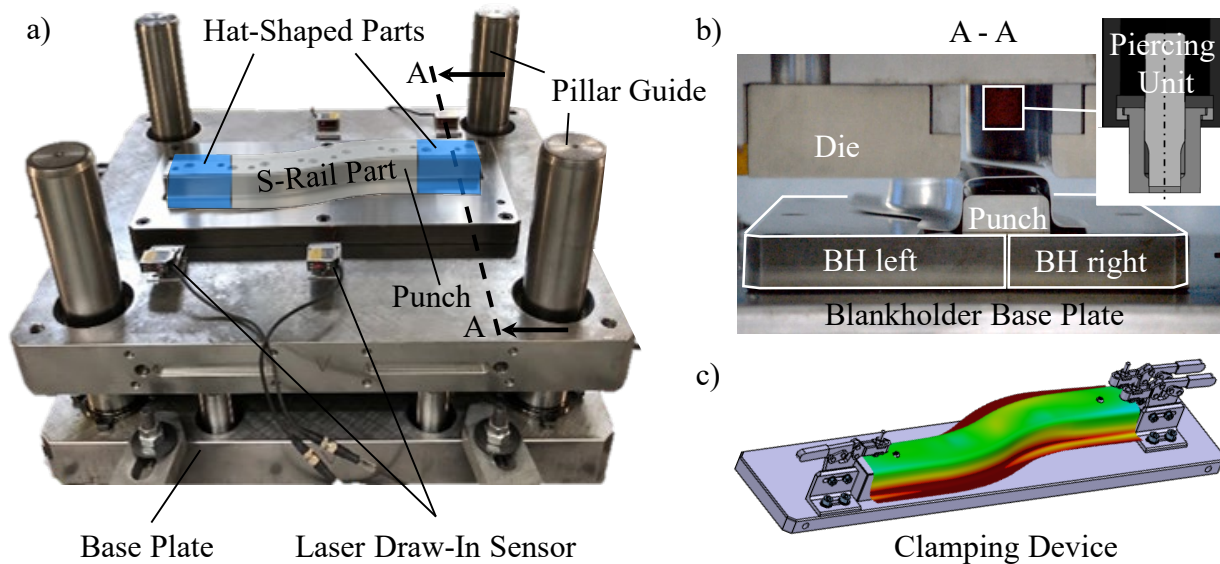


Fig. 4: Experimental setup for multistage deep-drawing with alternating blank draw-in.

The divided blankholder, in combination with different spacer heights, enables a differentiated leveling of the left and right drawing clearance between die and blankholder. With the spacer concept for the multistage deep-drawing with alternating blank draw-in, high loads on the pillar guides and inner tool bending moments due to an asymmetric tool tilt can be prevented (see Fig. 5). For this, spacer height and the opposite blankholder level is adjusted to achieve a parallel contact between blank, spacer and die. Specifically, the blankholder side, where draw-in of the blank is to be prevented by high friction controlled restraining forces, is raised by means of a foil shim that can be easily adjusted for different tool and process conditions. On the opposite side, where the draw-in of the blank should be enabled, spacer are placed along the blank edge between blankholder and die. The resulting gap reduces the tool-to-blank contact, thus reducing the friction controlled restraining force and enabling the asymmetric draw-in of the blank. The presented concept was applied to the existing prototype tool shown in Fig. 5, which was originally designed for conventional deep-drawing and springback investigations on high-strength steel material.

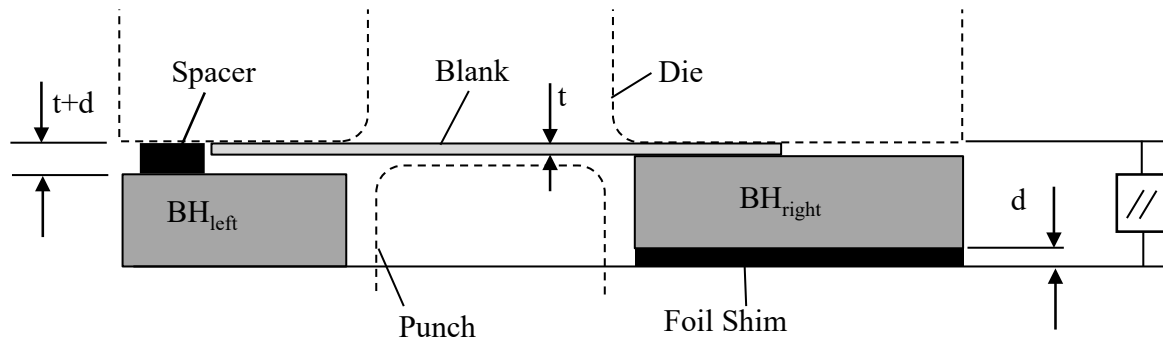


Fig. 5: Spacer concept to ensure asymmetric blank-draw-in and reduce the tool tilt.

Experimental Forming and Springback Results

In addition to the numerical findings, an experimental parameter study was elaborated to proof the springback compensation effect of deep-drawing with alternating draw-in. Here, by a variation of process parameters such as blankholder force, lubrication and spacer height, the numerically gathered sensitivity analysis was confirmed and extended with the definition of a feasible process window. All experiments were carried out on the AIDA 6300 servo-mechanical press of the IFU using the previously presented tool with the new spacer concept. First, rectangular blanks of DP980 steel grade were prepared in the dimensions of 160 mm length, 100 mm width and a blank thickness of 0.97 mm according to the numerical setup. By using these small blanks, which were formed to hat-shaped parts, a full-factorial testing of parameter sensitivity in a wide range of blankholder pressure was achieved. On each forming stroke, two blanks were deep-drawn with alternating blank draw-in within three forming operations and the proven beneficial drawing depth ratio of $i_{12} = 1.6$ (see Fig. 4). For the identification of the influence of blankholder force, lubrication and spacer height, the parameters were varied according to Table 2. The blankholder force was varied between 200 kN, which corresponds to an initial contact pressure of 11 MPa, and the maximum available blankholder force of 1500 kN (≈ 85 MPa). Prior to the forming experiments, blanks were manually cleaned and mineral oil M100 was precisely applied as lubricant. Beside a conventional amount of lubrication, further experiments with cleaned and dry formed blank material were performed to increase restraining forces. The impact of the spacer concept and its adjustable gap height was investigated by a variation of the spacer height between 1.02 mm and 1.27 mm for a blank thickness of 0.97 mm.

Table 2: Investigated parameter space of forming experiments with hat-shaped parts

Parameter	Range
Blankholder Force [kN]	200; 500; 1000; 1500
Lubrication [g/m ²]	0 (dry); 1.5; 3
Spacer height (t+d) [mm]	1.02; 1.07; 1.17; 1.27

The effect of each parameter variation on the alternating draw-in kinematic was tracked by using the installed displacement sensors. All parameter settings were repeated four times for a statistical evaluation. In doing so, the observed draw-ins and related scattering of the first two forming operations with alternating blank draw-in are illustrated over all parameter variations in Fig. 6 a). It was remarkable, that only a small spacer height (1.02 mm) was sufficient and led to the alternating draw-in kinematic. On contrary, further increasing of spacer height showed a neglectable impact on process robustness compared to the blankholder force. This parameter exhibits a strong influence on the process and ensures a robust prevention of draw-in on the clamping side at force values above 1000 kN. With a corresponding initial contact pressure of 57 MPa per flange area, the draw-in kinematic kept robustly constant for variable lubricated conditions and spacer heights. Furthermore, the experimental determined value corresponds in a good manner with the numerical pre-determined threshold (≈ 60 MPa). Blankholder forces above this value ensure a stable draw-in of 25 mm on each flange side, while preventing any draw-in on the opposite side. Symmetrical flange lengths after OP20 enable a successful final shape-set operation and ensure an efficient springback compensation. Nevertheless, process uncertainties indicated by the increase of scattering of draw-in values for operation 20 have to be mentioned because of the reduced flange length for clamping and preventing draw-in.

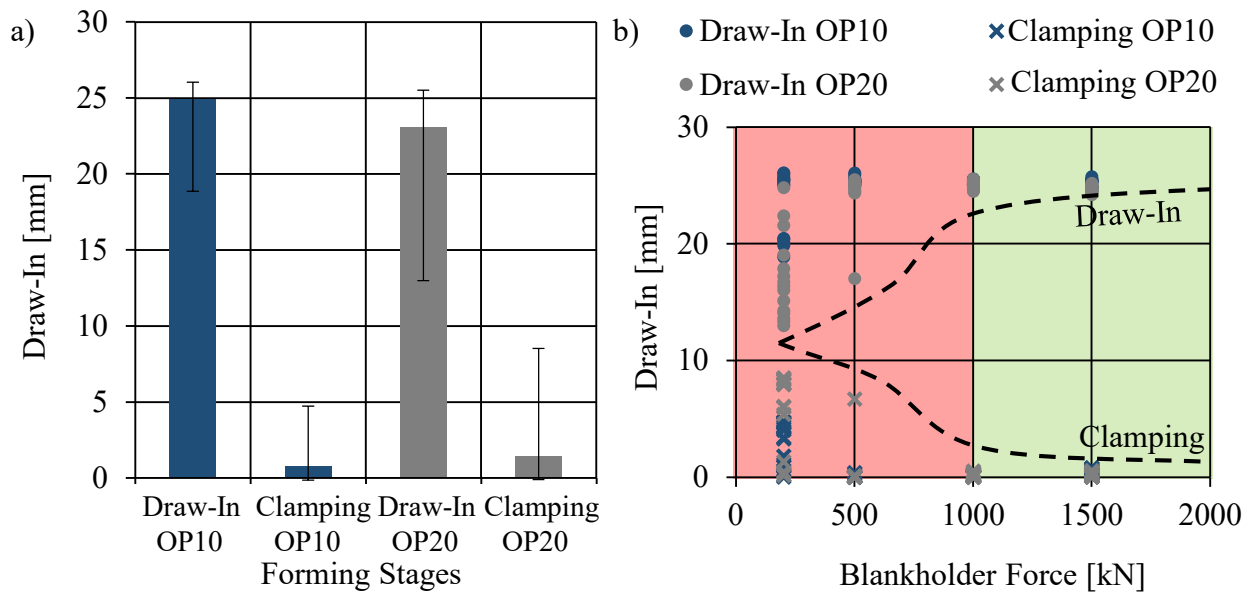


Fig. 6: Experimental observed draw-in for the first two operations over all parameter variations a) and for the dominant parameter blankholder force b)

In further forming experiments, gathered results and findings were finally transferred to an S-rail part geometry. The required S-shaped blanks having the dimensions 490 mm x 160 mm were separated from DP980 sheet metal by laser-cutting. Due to the enlargement of the part geometry, the available AIDA servo-mechanical press with its maximum of 1500 kN drawing cushion force only provided an initial blankholder pressure of 34 MPa. Therefore, blank draw-in on clamping sides was not fully prevented and other measures had to be considered. Only by using dry blanks without additional lubrication and a maximum spacer height of 1.27 mm, the required draw-in kinematic could be achieved. Thus, multistage deep-drawing with alternating blank draw-in could be successfully performed, considering a drawing depth ratio of $i_{12} = 1.6$. Fig. 7 shows the results of the surface comparison between original CAD data and measured springback geometry, scanned with optical 3D measuring device GOM ATOS 5M after each forming operation. After the first forming stage, high shape deformations can be observed in the flange and bottom area. The second forming operation with draw-in on the opposite flange side reduces the springback due to the counter bending of the material over tool radii. The superposition of stresses results in reduced shape deviations in the flange and part wall areas. The final shape-set operation mainly impacts the flatness of the part bottom area and reduces side wall curls. As a reference, conventional deep-drawing experiments with symmetric flange restraining forces by a total blankholder force of 1500 kN and 1.5 g/m² of lubricant M100 were carried out. Compared to the conventional drawn S-Rail part, deep-drawing with alternating blank draw-in reduces maximum springback in flange area by almost 75 % from 14.75 mm to 3.74 mm.

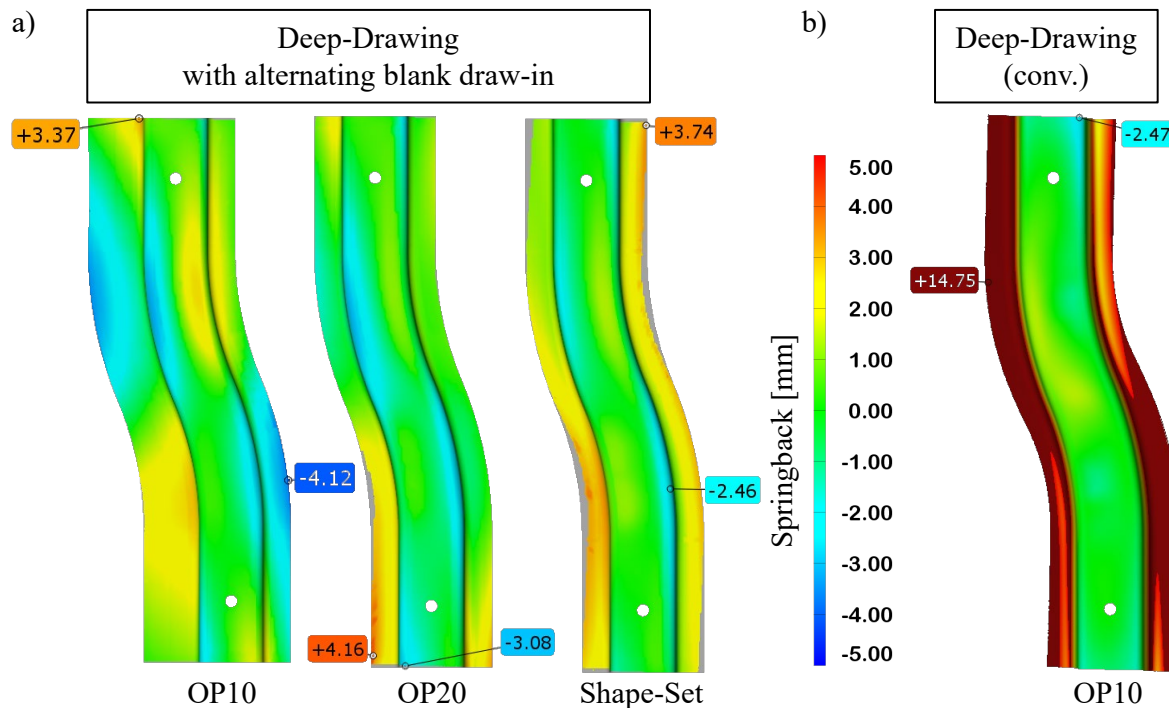


Fig. 7: Measured shape deviations for springback S-Rail geometry for experiments with a) deep-drawing with alternating blank draw-in and b) conventional deep-drawing

Summary

The numerical and experimental study presented in this paper demonstrates sensitivities of tool and process parameters of the new forming approach, multistage deep-drawing with alternating blank draw-in. Previous work on this field already showed a sufficient compensation effect by changing the draw-in direction within two operations and calibrate the final part geometry via shape-set operation. This demonstrates a compromise between sufficient alternated bending for stress superposition and therefore springback compensation but also taking the additional tooling cost into account by adding more forming operations [14]. For the investigations on this multiple forming process reported about in this paper, an enhanced material and simulation model was implemented in LS-DYNA to analyze influence of tool and process parameters such as tool radii and drawing depths on the forming result. Here, the drawing depth ratio i_{12} , which defines the relation between the drawing depths of the first two forming operations with alternating draw-in, showed a strong impact on draw-in kinematic and springback. The numerically identified ratio of $i_{12} = 1.6$ provided a beneficial and transferable process characteristic and ensured a symmetrical flange draw-in and robust springback results at the very end of the forming sequence.

The experimental section presented in this paper shows results of the forming processes of hat-shaped and S-Rail parts of DP980 steel sheets. Before that, a prototype tool was modified by a new spacer concept to enable asymmetric draw-in on one side and eliminate tool tilt and high loads on guiding components on the other side. A full-factorial experimental parameter study on the impact of blankholder force, lubrication and spacer height revealed parameter sensitivities on the alternating draw-in kinematic. Here, the blankholder force showed a dominant influence on the friction controlled alternating blank draw-in. The experimentally derived threshold value of an initial contact pressure to prevent draw-in on the clamping sides amounts 57 MPa and correlated well with the numerically determined value (≈ 60 MPa). By the application of high blankholder forces, a robust alternating draw-in kinematic and efficient springback compensation could be achieved. Further process parameters such as lubrication and spacer height appeared to be neglectable.

In future work, the efficient springback compensation by alternating bending over tool radii should be made accessible without high blankholder forces. Thus, an intelligent solution with controlled low-

friction blank draw-in may overcome present process limits and enhance the shape accuracy for cold forming of advanced high-strength steel sheets. Looking at available press technologies and tool space, deep-drawing with alternating draw-in within a single operation may reduce tooling cost and makes this new forming process industrial accessible.

Acknowledgement

The presented work was supported by the European Research Association for Sheet Metal Working (EFB 13/217) and the authors like to acknowledge the funding of the research project 20299N by the German Federation of Industrial Research Associations (AiF).

References

- [1] J. H. Schmitt and T. Iung, "New developments of advanced high-strength steels for automotive applications", *Comptes Rendus Phys.*, vol. 19, pp. 641–656, 2018.
- [2] N. Baluch, Z. Mohamed Udin and C. Sobry Abdullah, "Advanced High Strength Steel in Auto Industry: an Overview", *Eng. Appl. Sci. Res.*, vol. 4, no. 4, pp. 686–689, 2014.
- [3] S. Konzack, R. Radonjic, M. Liewald and T. Altan, "Prediction and reduction of springback in 3D hat shape forming of AHSS", *Procedia Manuf.*, vol. 15, pp. 660–667, 2018.
- [4] J. Naofal, H. M. Naeini and S. Mazdak, "Effects of hardening model and variation of elastic modulus on springback prediction in roll forming", *Metals (Basel)*, vol. 9, no. 9, pp. 1–13, 2019.
- [5] H. ul Hassan, F. Maqbool, A. Güner, A. Hartmaier, N. Ben Khalifa and A. E. Tekkaya, "Springback prediction and reduction in deep drawing under influence of unloading modulus degradation", *Int. J. Mater. Form.*, vol. 9, no. 5, pp. 619–633, 2016.
- [6] F. Yoshida and T. Uemori, "A model of large-strain cyclic plasticity and its application to springback simulation", *Int. J. Mech. Sci.*, vol. 45, pp. 1687–1702, 2003.
- [7] S. Toros, "Parameters Determination of Yoshida Uemori Model Through Optimization Process of Cyclic Tension-Compression Test and V-Bending Springback Abstract", *Lat. Am. J. Solids Struct.*, vol. 13, no. 10, pp. 1893–1911, 2016.
- [8] R. Neugebauer *et al.*, "Press hardening - An innovative and challenging technology", *Arch. Civ. Mech. Eng.*, vol. 12, pp. 113–118, 2012.
- [9] M. Kibben, L. Bode and T. Flehmig, "smartform ® by thyssenkrupp - Enhancement of production processes for a cost optimized cold forming of high strength steel", *Conf. "New Dev. Sheet Met. Forming"*, Stuttgart, pp. 87–96, 2018.
- [10] R. Radonjic and M. Liewald, "Forming with alternating blank draw-in as a new approach for springback reduction", *5th Int. Conf. Steels Cars Truck. Amsterdam*, 2017.
- [11] ISO 6892-1, "Metallic materials - Tensile testing - Part 1: Method of test at room temperature", *German version DIN EN ISO 6892-1*, 2020.
- [12] D. Briesenick, M. Liewald, R. Radonjic and C. Karadogan, "Enhanced accuracy in springback prediction for multistage sheet metal forming processes", *WGP-Jahreskongress, Hambg.*, pp. 111–120, 2019.
- [13] C. Lemieux, *Monte Carlo and Quasi-Monte Carlo Sampling*, Springer New York, 2009.
- [14] D. Briesenick and M. Liewald, "Rückfederungskompensation mittels Tiefziehens mit wechselseitigem Platineneinlauf", *EFB-Forschungsbericht Nr. 563*, 2021.